

Millimeter-wave Phase Noise Analysis on Period-one Dynamics in Semiconductor Lasers

Jun-Ping Zhuang¹, Song-Sui Li¹, Xiao-Zhou Li¹, and Sze-Chun Chan^{1,2,*}

¹Department of Electronic Engineering, City University of Hong Kong, Hong Kong, China

²State Key Laboratory of Millimeter Waves, City University of Hong Kong, Hong Kong, China

*Email: scchan@cityu.edu.hk

Abstract– Phase noise of the period-one (P1) nonlinear dynamics in a slave laser (SL) subject to injection from a master laser (ML) is analyzed via numerical simulations. The optical linewidth of the regeneration component is mainly determined by the ML linewidth, while the optical linewidth of the P1 component is dependent on both the ML and SL linewidths. The optical components in P1 dynamics are phase-correlated so that the microwave linewidth of the beat signal can be narrower than the optical linewidths, though the phase correlation degrades as the P1 oscillation frequency is tuned much beyond the relaxation resonance frequency of the laser.

1. Introduction

Nonlinear dynamics of semiconductor lasers have been of great interest due to the wide range potential photonic applications, including random bit generation [1], secure communication [2, 3], chaotic ranging [4-7], signal processing [8, 9], tunable microwave generation [10, 11], and radio-over-fiber communication [12, 13]. For photonic microwave generation, the period-one (P1) nonlinear dynamics in a slave laser (SL) subject to injection from a master laser (ML) have been intensively investigated. The generation technique based on the P1 dynamics has the advantages of wide frequency tunability, all-optical setup, and single side-band optical spectrum [14-17]. However, the stability of the microwave frequency is limited by the fluctuations in the lasers, which cause the phase noise in the P1 dynamics [18]. Recently, there are works focusing on the operating injection points, where the P1 oscillation frequency is insensitive to the variations of injection frequency and is consequently resistant some extent to the temperature fluctuations in the lasers [17, 19]. Complementary to these works, the intrinsic spontaneous emission noise in a laser is considered as the fundamental fluctuation source that corresponds to a non-zero optical linewidth in the injected laser. Considering only the spontaneous emission in the SL, the phase noise characteristics of the generated microwave signals also have been recently investigated numerically [20, 21], where optical feedback has been experimentally demonstrated for the phase noise reduction in the microwave signal generated by the P1 dynamics [14].

In this work, the spontaneous emission in both the ML and SL are considered. Their influence on the phase noise of the P1 dynamics are systematically investigated by numerical simulations, where the spontaneous emission is

modeled by a Langevin fluctuation force. To analyze the phase noise characteristics of the P1 dynamics, the ML and SL linewidths as well as the P1 oscillation frequency are varied. Meanwhile, the regeneration component's optical linewidth, P1 component's optical linewidth, and P1 microwave linewidth are simultaneously examined.

2. Simulation Model

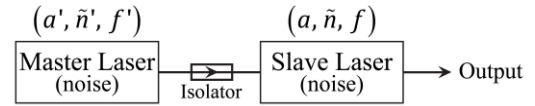


Fig. 1. Schematic of the SL subject to injection from the ML.

The schematic of the simulated setup is shown in Fig. 1. A continuous-wave light from the ML is delivered through an optical isolator and injected into the SL. Both the ML and SL are single-mode semiconductor lasers. The dynamical behavior of the SL and ML can be respectively described by the temporal evolution of state variables $(a(t), \tilde{n}(t))$ and $(a'(t), \tilde{n}'(t))$, where $a(t)$ and $a'(t)$ are the normalized complex intracavity optical field amplitudes, while $\tilde{n}(t)$ and $\tilde{n}'(t)$ are the normalized charge carrier densities [22]. When the SL is subject to an optical injection with the normalized injection strength ξ_i and the injection detuning frequency f_i , the SL dynamical behavior can be modeled by the following rate equations [20-22]:

$$\frac{da}{dt} = \frac{1 - ib}{2} \left[\frac{\gamma_c \gamma_n}{\gamma_s \bar{J}} \tilde{n} - \gamma_p (|a|^2 - 1) \right] a + \xi_i \gamma_c a'(t - \tau) e^{-i2\pi f_i t} + f, \quad (1)$$

$$\frac{d\tilde{n}}{dt} = -(\gamma_s + \gamma_n |a|^2) \tilde{n} - \gamma_s \bar{J} \left(1 - \frac{\gamma_p}{\gamma_c} |a|^2 \right) (|a|^2 - 1), \quad (2)$$

where, $\gamma_c = 5.36 \times 10^{11} \text{ s}^{-1}$ is the cavity decay rate, $\gamma_s = 5.96 \times 10^9 \text{ s}^{-1}$ is the spontaneous carrier relaxation rate, $\gamma_n = 7.53 \times 10^9 \text{ s}^{-1}$ is the differential carrier relaxation rate, $\gamma_p = 1.91 \times 10^{10} \text{ s}^{-1}$ is the nonlinear carrier relaxation rate, $\bar{J} = 1.222$ is the normalized bias current above threshold, and the linewidth enhancement factor $b = 3.2$ quantifies the dependence of the refractive index on the optical gain. The relaxation resonance frequency of the laser is $f_r = 10.25 \text{ GHz}$. The term with (ξ_i, f_i) in Eq. (1) represents the optical injection. In this term, $a'(t - \tau)$ is the normalized optical field amplitude from the ML with a delay τ . The ML, which is free-

running, can be modeled by another set of rate equations:

$$\frac{da'}{dt} = \frac{1 - ib'}{2} \left[\frac{\gamma'_c \gamma'_n}{\gamma'_s \tilde{J}'} \tilde{n}' - \gamma'_p (|a'|^2 - 1) \right] a' + f', \quad (3)$$

$$\frac{d\tilde{n}'}{dt} = -(\gamma'_s + \gamma'_n |a'|^2) \tilde{n}' - \gamma'_s \tilde{J}' \left(1 - \frac{\gamma'_p}{\gamma'_c} |a'|^2 \right) (|a'|^2 - 1), \quad (4)$$

where the parameters γ'_c , γ'_s , γ'_n , γ'_p , \tilde{J}' , and b' share the same values with the SL. In Eqs. (1) and (3), the Langevin fluctuation forces f and f' are included to model the intrinsic spontaneous emission noise in ML and SL, respectively. The Langevin fluctuation force f has the properties described by the following averages [18]:

$$\langle f(t) \rangle = 0, \quad (5)$$

$$\langle f(t) f(t') \rangle = 0, \quad (6)$$

$$\langle f(t) f^*(t') \rangle = \gamma_{sp} \delta(t - t'), \quad (7)$$

where γ_{sp} is proportional to the rate of the spontaneous emission. The force f' has the same properties as described by Eqs. (5)-(7) when f is replaced by f' and γ_{sp} is replaced by its γ'_{sp} . The different values of γ_{sp} and γ'_{sp} characterize the noise strengths resulting in different laser linewidths in the SL and ML, respectively. For numerical simulation, the second-order Runge-Kutta integration on Eqs. (1)-(4) is conducted with a time step of 0.95 ps and an effective time span of 16.4 μ s. To extract the linewidth values, the obtained optical spectra and power spectra are fitted with a Lorentzian lineshape.

3. Noise Sources

In Fig. 2, the influence of different noise sources on the P1 dynamics is investigated. The noise strength is kept constant so that the free-running laser linewidth is 9.1 MHz when the corresponding laser noise is included. The SL is optically injected at $(\xi_i, f_i) = (0.174, 14.5 \text{ GHz})$ so that it is driven into P1 dynamics with an oscillation frequency of $f_0 = 24 \text{ GHz}$.

Figure 2(a-i) shows the optical spectrum of the P1 oscillation without any noise. The optical spectrum is dominated by the regeneration component at the offset frequency of f_i indicated by the downward arrow and the P1 component at the offset frequency of $f_i - f_0$. These two components are over 10 dB stronger than the others. Because no noise is included, the regeneration component's optical linewidth $\Delta\nu_i$ and P1 component's optical linewidth $\Delta\nu_0$ are both narrower than the simulation's spectral resolution. Therefore, the beat signal of the optical components also exhibits nearly no microwave linewidth Δf_0 at the frequency of $f_0 = 24 \text{ GHz}$ as the power spectrum in Fig. 2(a-ii) shows.

In Fig. 2(b), the noise in the SL is included, while the noise in the ML is neglected. Although the regeneration component's linewidth $\Delta\nu_i$ is still narrower than the spectral resolution of the simulation, the P1 component's linewidth broadens to $\Delta\nu_0 = 2.3 \text{ MHz}$. However, it is narrower than the free-running SL linewidth of $\Delta\nu_{SL} = 9.1 \text{ MHz}$. The narrow linewidth $\Delta\nu_0$ is attributed to

the nonlinear frequency mixing among a number of optical frequency components in Fig. 2(b-i) [20]. The P1 microwave linewidth also broadens to $\Delta f_0 = 2.3 \text{ MHz}$ with the same value as $\Delta\nu_0$, as Fig. 2(b-ii) shows.

In contrast to Fig. 2(b), the ML noise is included, while the SL noise is neglected in Fig. 2(c). As shown in Fig. 2(c-i), the regeneration component's linewidth broadens to $\Delta\nu_i = 9.1 \text{ MHz}$, which is the same as the free-running ML linewidth $\Delta\nu_{ML}$. The P1 component's linewidth broadens, as well, to $\Delta\nu_0 = 5.5 \text{ MHz}$. The broadening of $\Delta\nu_0$ implies that the phase noise in the injection frequency f_i can be coupled to the P1 component at the frequency of $f_i - f_0$ in Fig. 2(c-i). The P1 microwave linewidth is $\Delta f_0 = 2.8 \text{ MHz}$ as shown in Fig. 2(c-ii). It is worth noting that Δf_0 is narrower than both the optical linewidths of $\Delta\nu_i$ and $\Delta\nu_0$, indicating the phase correlation between the optical components of the P1 dynamics in Fig. 2(c-i).

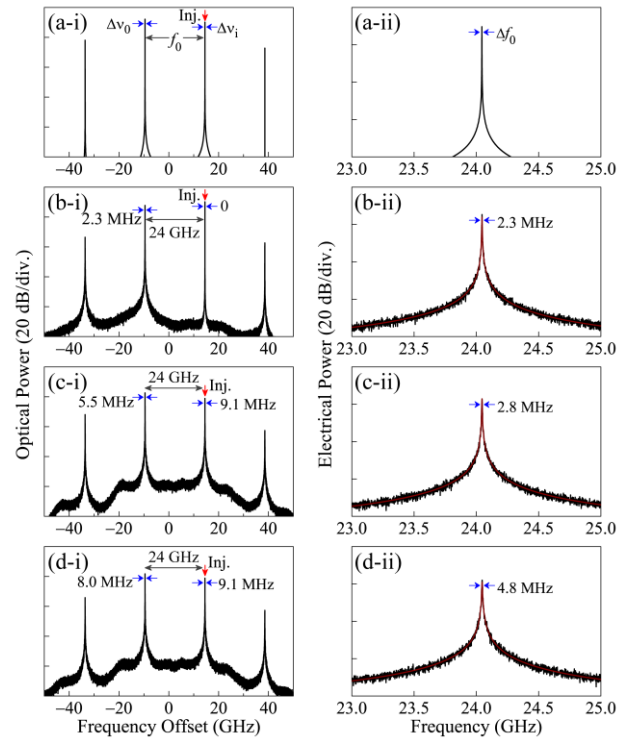


Fig. 2. (i) Optical spectra and (ii) power spectra of the SL emission subject to an optical injection of $(\xi_i, f_i) = (0.174, 14.5 \text{ GHz})$ with different noise sources: (a) no noise, (b) noise in SL alone, (c) noise in ML alone, and (d) noise in both SL and ML. The noise strengths correspond to an optical linewidth of 9.1 MHz for the free-running lasers. The frequency axis of the optical spectrum is offset to the free-running SL frequency.

In Fig. 2(d), the noise in both the ML and the SL are included so that the free-running linewidths of both $\Delta\nu_{ML}$ and $\Delta\nu_{SL}$ are 9.1 MHz. As a result, the regeneration component has linewidth $\Delta\nu_i = 9.1 \text{ MHz}$, while the P1 component has linewidth further broadened to $\Delta\nu_0 = 8.0 \text{ MHz}$, as Fig. 2(d-i) shows. Accordingly, the microwave linewidth broadens to $\Delta f_0 = 4.8 \text{ MHz}$ as Fig. 2(d-ii) shows. Again, the microwave linewidth Δf_0 is

narrower than both Δv_i and Δv_0 in the P1 dynamics.

In short, the regeneration component's linewidth Δv_i is always the same as the free-running ML linewidth Δv_{ML} , while the P1 component's linewidth Δv_0 is dependent on both Δv_{SL} and Δv_{ML} . Moreover, the beat signal linewidth Δf_0 can be narrower than the optical linewidths Δv_i and Δv_0 in the P1 dynamics.

4. P1 Microwave Linewidth Δf_0

In this section, the noise strengths in ML and SL are separately tuned so that the free-running laser linewidths Δv_{ML} and Δv_{SL} are varied accordingly. Then, the dependence of the P1 dynamical linewidths Δv_i , Δv_0 , and Δf_0 on the free-running laser linewidths Δv_{ML} and Δv_{SL} are investigated.

4.1 Dependence on Master Laser Linewidth Δv_{ML}

In Fig. 3, the P1 dynamical linewidths Δv_i , Δv_0 , and Δf_0 are shown as the ML linewidth Δv_{ML} is varied from $\Delta v_{ML} = 1.2$ MHz to 90 MHz. The free-running SL linewidth is kept at $\Delta v_{SL} = 9.1$ MHz. The regeneration component's linewidth Δv_i is essentially equal to the ML linewidth Δv_{ML} as shown by the squares in Fig. 3. As the diamonds in Fig. 3 show, the P1 component's linewidth Δv_0 increases with Δv_{ML} , indicating that the phase noise in the injection light is coupled to the P1 component. Correspondingly, the P1 microwave linewidth Δf_0 also increases with Δv_{ML} as shown by the circles in Fig. 3. Moreover, the P1 microwave linewidth Δf_0 (circles) is always narrower than the P1 component's linewidth Δv_0 (diamonds) implying that the P1 component is phase correlated with the regeneration component. Actually, both the phase noise coupling and the phase correlation stem from the nonlinear coupling between the optical gain and the refractive index of gain medium [20, 22].

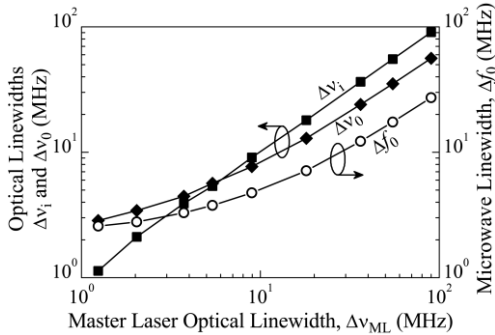


Fig. 3. Optical linewidth (closed symbols) and microwave linewidth (open symbols) as functions of the ML optical linewidth Δv_{ML} . Squares, regeneration component's linewidth Δv_i ; diamonds, P1 component's optical linewidth Δv_0 ; open circles, P1 microwave linewidth Δf_0 .

4.2 Dependence on Slave Laser Linewidth Δv_{SL}

Figure 4 illustrates the influence of the free-running SL linewidth Δv_{SL} on the P1 dynamical linewidths Δv_i , Δv_0 , and Δf_0 . In contrast to Section 4.1, the free-running SL linewidth is varied from $\Delta v_{SL} = 1.2$ MHz to 90 MHz, while the ML linewidth is kept constant at $\Delta v_{ML} = 9.1$ MHz. As the squares in Fig. 4 show, the

regeneration component's linewidth Δv_i is constant as Δv_{SL} varies, indicating that Δv_i is fully determined by the ML linewidth Δv_{ML} . Again, the P1 microwave linewidth Δf_0 (circles) is narrower than the P1 component's linewidth Δv_0 (diamonds). As Δv_{SL} increases, both Δv_0 and Δf_0 are broadened at the same time.

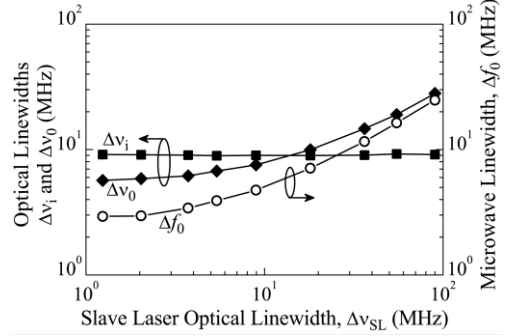


Fig. 4. Optical linewidth (closed symbols) and microwave linewidth (open symbols) as functions of the free-running SL optical linewidth Δv_{SL} . Squares, regeneration component's linewidth Δv_i ; diamonds, P1 component's optical linewidth Δv_0 ; open circles, P1 microwave linewidth Δf_0 .

4.3. Dependence on P1 Oscillation Frequency f_0

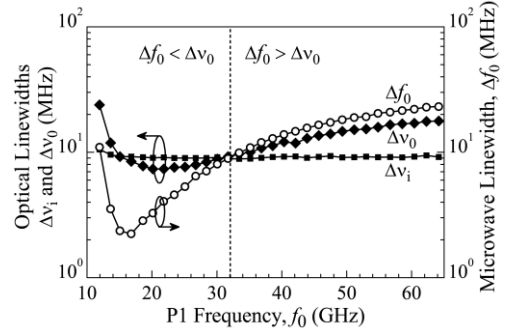


Fig. 5. Optical linewidth (closed symbols) and microwave linewidth (open symbols) as functions of the P1 oscillation frequency f_0 . Squares, regeneration component's linewidth Δv_i ; diamonds, P1 component's optical linewidth Δv_0 ; open circles, P1 microwave linewidth Δf_0 .

In Fig. 5, the P1 dynamical linewidths Δv_i , Δv_0 , and Δf_0 are examined as the P1 oscillation frequency f_0 is varied from around the relaxation resonance frequency $f_r = 10.25$ GHz to over 64 GHz in the millimeter wave regime. For tuning the P1 frequency f_0 , the injection parameters are chosen in such a way that the microwave power is maximal. The free-running laser linewidths of Δv_{ML} and Δv_{SL} are both kept constant at 9.1 MHz. As shown by the squares in Fig. 5, the regeneration component's linewidth Δv_i is almost unchanged as the P1 frequency f_0 is varied. Again, the P1 component's linewidth Δv_0 (diamonds) and P1 microwave linewidth Δf_0 (circles) follow the similar trend that the linewidth broadens as f_0 is tuned much beyond f_r . However, there are two different regimes with $\Delta f_0 < \Delta v_0$ and $\Delta f_0 > \Delta v_0$, which are separated by the dashed line in Fig. 5. The increment of $\Delta f_0 - \Delta v_0$ implies that the phase correlation between the optical components degrades as f_0 increases much beyond f_r . Also, as f_0 approaches f_r , Fig. 5 shows a sharp increase

of $\Delta\nu_0$ and Δf_0 due to the proximity to the emergence of other nonlinear dynamics [14, 20].

5. Conclusion

In conclusion, the intrinsic laser noise in both ML and SL are considered on the phase noise characteristics of the P1 dynamics numerically. The phase noise of the P1 dynamics is analyzed by simultaneously examining the P1 dynamical linewidths $\Delta\nu_i$, $\Delta\nu_0$, and Δf_0 . The regeneration component's linewidth $\Delta\nu_i$ is determined by $\Delta\nu_{ML}$ alone, while the P1 component's linewidth $\Delta\nu_0$ is dependent on both $\Delta\nu_{ML}$ and $\Delta\nu_{SL}$. The P1 microwave linewidth Δf_0 can be narrower than the optical linewidths indicating the phase correlation between the optical components in the P1 dynamics, though the phase correlation degrades as the P1 frequency f_0 is tuned much beyond f_r .

Acknowledgments

The work described in this paper was fully supported by a grant from the Research Grants Council of Hong Kong, China (Project No. CityU 11201014).

References

- [1] A. Uchida, K. Amano, M. Inoue, K. Hirano, S. Naito, H. Someya, I. Oowada, T. Kurashige, M. Shiki, S. Yoshimori, K. Yoshimura, and P. Davis, "Fast physical random bit generation with chaotic semiconductor lasers," *Nat. Photon.*, vol. 2, pp. 728–732, 2008.
- [2] M. Sciamanna and K.A. Shore, "Physics and applications of laser diode chaos," *Nat. Photon.*, vol. 9, pp. 151–162, 2015.
- [3] M.C. Soriano, J. Garcia-Ojalvo, C.R. Mirasso, and I. Fischer, "Complex photonics: Dynamics and applications of delay-coupled semiconductor lasers," *Rev. Mod. Phys.*, vol. 85, pp. 421–470, 2013.
- [4] F.Y. Lin and J.M. Liu, "Chaotic lidar," *IEEE J. Sel. Topics Quantum Electron.*, vol. 10, pp. 991–997, 2004.
- [5] S.D. Cohen, A. Aragoneses, D. Rontani, M. Torrent, C. Masoller, and D.J. Gauthier, "Multidimensional subwavelength position sensing using a semiconductor laser with optical feedback," *Opt. Lett.*, vol. 38, pp. 4331–4334, 2013.
- [6] M. Zhang, Y. Ji, Y. Zhang, Y. Wu, H. Xu, and W. Xu, "Remote radar based on chaos generation and radio over fiber," *IEEE Photon. J.*, vol. 6, pp. 1–12, 2014.
- [7] C.H. Cheng, L.C. Lin, and F.Y. Lin, "Self-mixing dual-frequency laser Doppler velocimeter," *Opt. Express*, vol. 22, pp. 3600–3610, 2014.
- [8] S.C. Chan, Q. Liu, Z. Wang, and K.S. Chiang, "Tunable negative-tap photonic microwave filter based on a cladding-mode coupler and an optically injected laser of large detuning," *Opt. Express*, vol. 19, pp. 12 045–12052, 2011.
- [9] Y.H. Hung, C.H. Chu, and S.K. Hwang, "Optical double-sideband modulation to single-sideband modulation conversion using period-one nonlinear dynamics of semiconductor lasers for radio-over-fiber links," *Opt. Lett.*, vol. 38, pp. 1482–1484, 2013.
- [10] S.C. Chan and J.M. Liu, "Tunable narrow-linewidth photonic microwave generation using semiconductor laser dynamics," *IEEE J. Sel. Topics Quantum Electron.*, vol. 10, pp. 1025–1032, 2004.
- [11] J.P. Zhuang and S.C. Chan, "Tunable photonic microwave generation using optically injected semiconductor laser dynamics with optical feedback stabilization," *Opt. Lett.*, vol. 38, pp. 344–346, 2013.
- [12] C.C. Cui, X.L. Fu, and S.C. Chan, "Double-locked semiconductor laser for radio-over-fiber uplink transmission," *Opt. Lett.*, vol. 34, pp. 3821–3823, 2009.
- [13] C.C. Cui and S.C. Chan, "Performance analysis on using period-one oscillation of optically injected semiconductor lasers for radio-over-fiber uplinks," *IEEE J. Quantum Electron.*, vol. 48, pp. 490–499, 2012.
- [14] S.C. Chan, S.K. Hwang, and J.M. Liu, "Period-one oscillation for photonic microwave transmission using an optically injected semiconductor laser," *Opt. Express*, vol. 15, pp. 14 921–14935, 2007.
- [15] N.A. Naderi, M. Pochet, F. Grillot, N.B. Terry, V. Kovanis, and L.F. Lester, "Modeling the injection-locked behavior of a quantum dash semiconductor laser," *IEEE J. Sel. Topics Quantum Electron.*, vol. 15, pp. 563–571, 2009.
- [16] A. Hurtado, J. Mee, M. Nami, I.D. Henning, M.J. Adams, and L.F. Lester, "Tunable microwave signal generator with an optically-injected 1310 nm QD-DFB laser," *Opt. Express*, vol. 21, pp. 10 772–10778, 2013.
- [17] T.B. Simpson, J.M. Liu, M. AlMulla, N.G. Usechak, and V. Kovanis, "Limit-cycle dynamics with reduced sensitivity to perturbations," *Phys. Rev. Lett.*, vol. 112, p. 023901, 2014.
- [18] C. Henry, "Phase noise in semiconductor lasers," *J. Lightwave Technol.*, vol. 4, pp. 298–311, 1986.
- [19] T.B. Simpson, J.M. Liu, M. AlMulla, N.G. Usechak, and V. Kovanis, "Linewidth sharpening via polarization-rotated feedback in optically injected semiconductor laser oscillators," *IEEE J. Sel. Topics Quantum Electron.*, vol. 19, p. 1500807, 2013.
- [20] J.P. Zhuang and S.C. Chan, "Phase noise characteristics of microwave signals generated by semiconductor laser dynamics," *Opt. Express*, vol. 23, pp. 2777–2797, 2015.
- [21] K.H. Lo, S.K. Hwang, and S. Donati, "Optical feedback stabilization of photonic microwave generation using period-one nonlinear dynamics of semiconductor lasers," *Opt. Express*, vol. 22, pp. 18 648–18661, 2014.
- [22] S.C. Chan, "Analysis of an optically injected semiconductor laser for microwave generation," *IEEE J. Quantum Electron.*, vol. 46, pp. 421–428, 2010.